



# Biodistribution and Non-linear Gene Expression of mRNA LNPs Affected by Delivery Route and Particle Size

Jiaxing Di<sup>1</sup> · Zhili Du<sup>2</sup> · Kangzeng Wu<sup>3</sup> · Shanshan Jin<sup>3</sup> · Xun Wang<sup>2</sup> · Tonglei Li<sup>4</sup> · Yuhong Xu<sup>1,2,3</sup>

Received: 9 November 2021 / Accepted: 10 January 2022 / Published online: 26 January 2022  
© The Author(s), under exclusive licence to Springer Science+Business Media, LLC, part of Springer Nature 2022

## ABSTRACT

**Purpose** Lipid nanoparticles (LNPs) are widely utilized as means to deliver mRNA molecules. However, metric connections between biodistribution and pharmacokinetics (PK) of the nanoparticle carrier and transgene expression dynamics remain largely unknown.

**Methods** LNPs containing mRNAs encoding the firefly luciferase gene were prepared with varying sizes. Biodistributions of injected LNPs in mice were measured by fluorescence bioimaging or liquid chromatography with tandem mass spectrometry. In addition, luciferase expression levels were determined by bioluminescence imaging and enzyme activity assays.

**Results** Some intramuscularly injected LNPs were found circulating in the system, resulting in accumulation in the liver and spleen, especially when the LNP sizes were relatively small. Bigger LNPs were more likely to remain at the injection site. Transgene expression in the liver was found most prominent compared with other organs and tissues.

**Conclusions** Biomolecules such as mRNAs encapsulated in locally injected LNPs can reach other organs and tissues via systemic circulation. Gene expression levels are affected by the LNP biodistribution and pharmacokinetics (PK), which are

further influenced by the particle size and injection route. As transfection efficiency varies in different organs, the LNP exposure and mRNA expression are not linearly correlated.

**KEY WORDS** distribution · lipids nanoparticle · mRNA · transfection luciferase

## INTRODUCTION

A messenger RNA (mRNA) can encode a protein leading to desired biological functions, supporting the rationale for developing mRNA-based therapeutics (1–6). Recently, the mRNA vaccine field has progressed extremely rapidly, led by the successful approval and wide use of COVID-19 mRNA vaccines that encode the viral spike protein genes (7,8). The vaccines are formulated as lipid nanoparticles (LNPs), and the clinical acceptance of LNPs has been ushering the delivery system for various therapeutic applications in many disease areas.

LNPs are usually prepared using four lipid components: cationic lipids, phosphatidylcholines, cholesterol, and PEG-lipids. The cationic lipids become ionizable at lower physiological pH, for example, pH 4.0, and remain neutral at pH 7.4. The lipid compositions and their complexation methods with mRNAs had been studied extensively, and several studies were published about the formulation development of COVID-19 mRNA vaccines (2,9). However, most reports focused on the immune response and its pharmacodynamics (PD) by measuring the neutralizing antibody titers and T cell immunities. There have been few studies on the pharmacokinetics (PK) and biodistribution of LNPs and, more importantly, subsequent influence on the distribution and kinetics of the resulting gene products. In a recent report, transgene expression kinetics resulting from mRNA LNPs delivery via six different routes were investigated, but the PK of LNPs themselves was not included (10). In another report, possible

✉ Tonglei Li  
tonglei@purdue.edu

✉ Yuhong Xu  
yhxu@dali.edu.cn

<sup>1</sup> School of Pharmacy, Shanghai Jiao Tong University, Shanghai, China

<sup>2</sup> School of Pharmacy, Dali University, Dali Bai Autonomous Prefecture, Dali, China

<sup>3</sup> College of Pharmaceutical Sciences, Zhejiang University, Hangzhou, China

<sup>4</sup> Department of Industrial and Physical Pharmacy, Purdue University, RHPH Building, RM 124, 575 Stadium Mall Dr, West Lafayette, Indiana 47907, USA

connections between the size of LNPs and the induced immune response were discussed, but the underlying linkage or cause was not addressed (11).

Understanding the PK-PD relationship of an LNP-based mRNA delivery system is imperative to further mRNA applications in gene therapy. *In vivo* exposure of LNPs precedes gene expression from the delivered mRNA. However, the exposure and response kinetics are not necessarily directly associated. Some injected mRNA LNPs may migrate from the injection site and dispose to other tissues in the body, their integrity and transfection efficiency towards different cell types would significantly impact transgene expression in various tissues. While myocytes are thought to be the main target of intramuscularly injected LNPs, transgene expression in the liver has been observed (10). As such, this study examined the PK and biodistribution of LNPs containing mRNAs, which encode the firefly enzyme luciferase and are mostly intracellularly expressed and systemically non-immunogenic. Luciferase activities were measured from the perspective of pharmacodynamic evaluation. Additionally, ovalbumin-coded mRNA (OVAL) was used in our study of the cellular distribution of mRNAs. LNPs of varying sizes were prepared under different mixing concentrations. Biodistribution and PK of the LNPs and the resulting luciferase activities were analyzed in a murine model. Our results indicate a non-linear relationship between the exposure of LNPs and transgene expression dynamics.

## MATERIALS AND METHODS

### Materials

Hydrogenated soybean phosphatidylcholine (HSPC) was purchased from Lipoid (Newark, USA). Cholesterol was from Nippon Fine Chemical (Osaka, Japan). Deuterated cholesterol was from Cambridge Isotope Laboratories (Tewksbury, USA). 1,2-dimyristoyl-rac-glycero-3-methoxypolyethylene glycol-2000 (DMG-PEG2000) was from A.V.T. (Shanghai, China). (6Z,9Z,28Z,31Z)-heptatriaconta-6,9,28,31-tetraeb-19-Y13-(4-methylpiperazin-1-Y1) propanoate (H3) was synthesized by BirdoTech (Shanghai, China) (6). EZ Cap™ firefly luciferase mRNA was provided by ApexBio (Houston, USA). 1,1-dioctadecyl-3,3,3,3-tetramethylindotricarbocyanine iodide (DiR) and luciferin were obtained from Yeasen (Shanghai, China). Water used through experiments was purified using a Millipore Milli-Q purification system (Bedford, MA). All other reagents were of chemical purity or analytical grade from Sangon Biotech (Shanghai, China).

For the synthesis of OVAL mRNA used in the *in-situ* hybridization (ISH) study, we used the T7 high yield RNA transcription kit from Novoprotein (Shanghai, China) and performed *in vitro* transcription (IVT) of a linearized DNA

template from plasmid pCl-neo-sOVA (Addgene, Watertown, USA). The RNA was capped and attached poly(A) tails using enzymes included in the kit (Novoprotein, Shanghai, China).

### LNP Preparation

Lipids were dissolved in ethanol, including an ionizable lipid (H3), hydrogenated soy phosphatidylcholine (HSPC), cholesterol, and 1,2-dimyristoyl-rac-glycero-3-methoxypolyethylene glycol-2000 (DMG-PEG 2000) at the molar ratio of 19.5:14:64:2.5. The ratios were set based on earlier studies using H3 which has two ionizable tertiary amines per molecule (data not presented). For preparing fluorescence-labeled LNPs or deuterated cholesterol labeled LNPs, DiR or deuterated cholesterol were added into the lipids in ethanol at about 1% mol or 3.5% mol, respectively. LNPs were prepared based on a modified ethanol injection procedure (12). Briefly, the lipid mixtures in ethanol were rapidly injected into 10 mM citrate buffer (pH 4.0) containing mRNAs to a final phosphate to nitrogen molar ratio of 1:7. The mixtures were dialyzed against HEPES (pH 7.4) in a 100,000 MWCO cassette at 4°C overnight. For preparing LNPs with different particle sizes, the volume ratio of alcohol to water during mixing was adjusted to 1:5, 1:4, 1:3, while the mRNA concentrations used were 0.2 mg/mL, 0.3 mg/mL, 0.4 mg/mL respectively.

### LNP Characterization

The hydrodynamic size distribution, polydispersity (PDI), and zeta potential of the mRNA LNPs were obtained using a Zetasizer Nano ZS (Malvern Instrument, UK) after dilution in ultrapure water. The mRNA encapsulation status was examined by gel electrophoresis on a 1% agarose gel (30 min, 110 V) in MOPS (3-N(morpholino) propanesulfonic acid) buffer containing the GelRed dye. The samples include naked mRNA, the LNPs, LNPs in 10% Triton X-100, and the MW markers.

For the cryoEM examination, a sample of 3 μL of the LNP solution was deposited onto a glow-discharged lacey carbon grid (Quantifoil R1.2/1.3) and vitrified using a Vitrobot Mark IV (Thermo Fisher Scientific, Hillsboro, USA). The EM images were obtained on a Talos F200C Electron Microscope equipped with a Ceta 4 k × 4 k camera running at an accelerating voltage of 200 kV.

### Cell Transfection

HEK293T cells were maintained at 37°C under 5% CO<sub>2</sub> atmosphere in RPMI 1640 medium supplemented with 10% fetal bovine serum and 1% penicillin plus streptomycin. Cells were seeded in 24-well plates at a density of 250,000 cells

per well. After 24 h, they were transfected using LNPs containing the luciferase mRNA at various concentrations (0.5  $\mu$ g, 1  $\mu$ g, or 2  $\mu$ g). At specific time points (1 h, 4 h, 7 h, 24 h, 48 h) after the LNP addition, cells were lysed and analyzed for protein expression using the Luciferase Assay Kit (Beyotime, Shanghai, China).

### Animal Transfection Studies

All animal procedures in the study were performed according to the protocol approved by the Zhejiang University Institutional Animal Care and Use Committee (IACUC). As the gender of animals might not play a role in affecting the biodistribution and PK of our nanoparticles, only female mice were chosen in the study. Further studies with male mice will be conducted to validate our current results. Female BALB/c mice aged 6–8 weeks ( $n = 3$  per group) received DiR, or  $^2\text{H}$ -labeled cholesterol labeled LNPs containing 10  $\mu$ g of mRNA via intramuscular (i.m.), subcutaneous (s.c.), or intravenous(i.v.) routes, respectively. At 0.5, 1, 2, 4, 6, 10, and 24 h after the injection, blood samples were collected in the anticoagulant tube and stored at  $-80^\circ\text{C}$ . In addition, tissue samples from respectively euthanized animals, including liver, spleen, muscle, and lymph node were collected at 2, 6, 10, 24 h after injection of mRNA LNP. The protein expression levels in the collected blood and tissue samples were analyzed in the same way aforementioned.

To further observe the signal value of a specific organ, tissues including liver, spleen, muscle, and lymph node were collected immediately, and luminescence and fluorescence signals of the tissue samples were measured by IVIS® Spectrum (PerkinElmer, Waltham, USA).

With the animals euthanized, the deuterated cholesterol quantities in dissected plasma, liver, spleen, and muscle samples at pre-determined time points were analyzed by QTRAP® 5500 LC-MS/MS (SCIEX, Framingham, USA).

### Live Animal Imaging

Female BALB/c mice injected with DiR labeled mRNA LNPs described above were anesthetized and placed in an IVIS® Spectrum (PerkinElmer, Waltham, USA). The DiR fluorescence images were taken under the excitation and emission wavelengths of 745 and 800 nm, respectively. For the bioluminescence imaging, the animals were injected with the luciferase substrate luciferin, followed by imaging 3 min later in the IVIS® Spectrum. The luminescence or fluorescence intensities in each region of interest (ROIs) were quantified using the Living Image 3.0 software (PerkinElmer, Waltham, USA).

### RNA *In Situ* Hybridization (ISH) Assay

Various tissue samples were collected from euthanized animals and fixed in formalin. Formalin-fixed paraffin-embedded tissue sections were deparaffinized using gradient alcohol and digested with protease. The samples were then hybridized with the RNA probe. Finally, the tissue was counterstained with DAPI and observed with an Eclipse Ni-E upright fluorescence microscope (Nikon, Tokyo, Japan).

### Statistical Analysis

Statistical analysis was done using Prism 8.0 (GraphPad, San Diego, USA). Unless specified, data are presented as mean  $\pm$  standard deviation. T- test was used to compare the statistical differences between the naked mRNA group and mRNA LNP group in Figs. 1 and 4 (\*\*:  $p < 0.01$ ; \*\*\*:  $p < 0.001$ ; \*\*\*\*:  $p < 0.0001$ ).

## RESULTS

### Physical and Biological Evaluations of Fluc-mRNA LNPs

Fluc-mRNA LNPs were prepared by ethanol injection of the lipid mixture into the aqueous solution of mRNAs under various mixing conditions. The resulted LNP structures varied with the mRNA concentration during mixing and the ethanol to buffer ratio. Figure 1A listed three different scenarios, whereas the particle sizes were categorized as small, medium, or large. The cryoEM images of the LNPs revealed several different microstructures. Since only lipid bilayers are easily visible, we can differentiate them into single bilayer structures and multi-layer structures. The small-sized LNP preparation contained mostly the single bilayer structures, while the large-sized LNP preparation contained multi-layer structures. The medium-sized LNP preparation contained both.

The medium sized LNP preparations were utilized in most of our studies unless otherwise specified. Gel electrophoresis was used to demonstrate that mRNAs were packed in the LNPs (Fig. 1B). There was no detectable free mRNA in the LNP column, but the mRNAs were visible after the LNPs were partially dissociated by Triton-X treatment. The Fluc-mRNA LNPs were applied to HEK293T cells for evaluation of transfection (Figs. 1C-E). The mRNA-packed LNPs led to significantly higher gene expression compared to the same dose of mRNA by itself (Fig. 1C). The gene expression could be detected just 1 h after the LNP application but peaked at around 24 h (Fig. 1D). There was a clear dose correlation between the gene expression levels and the mRNA dose in the LNPs in cell transfection experiments (Fig. 1E).

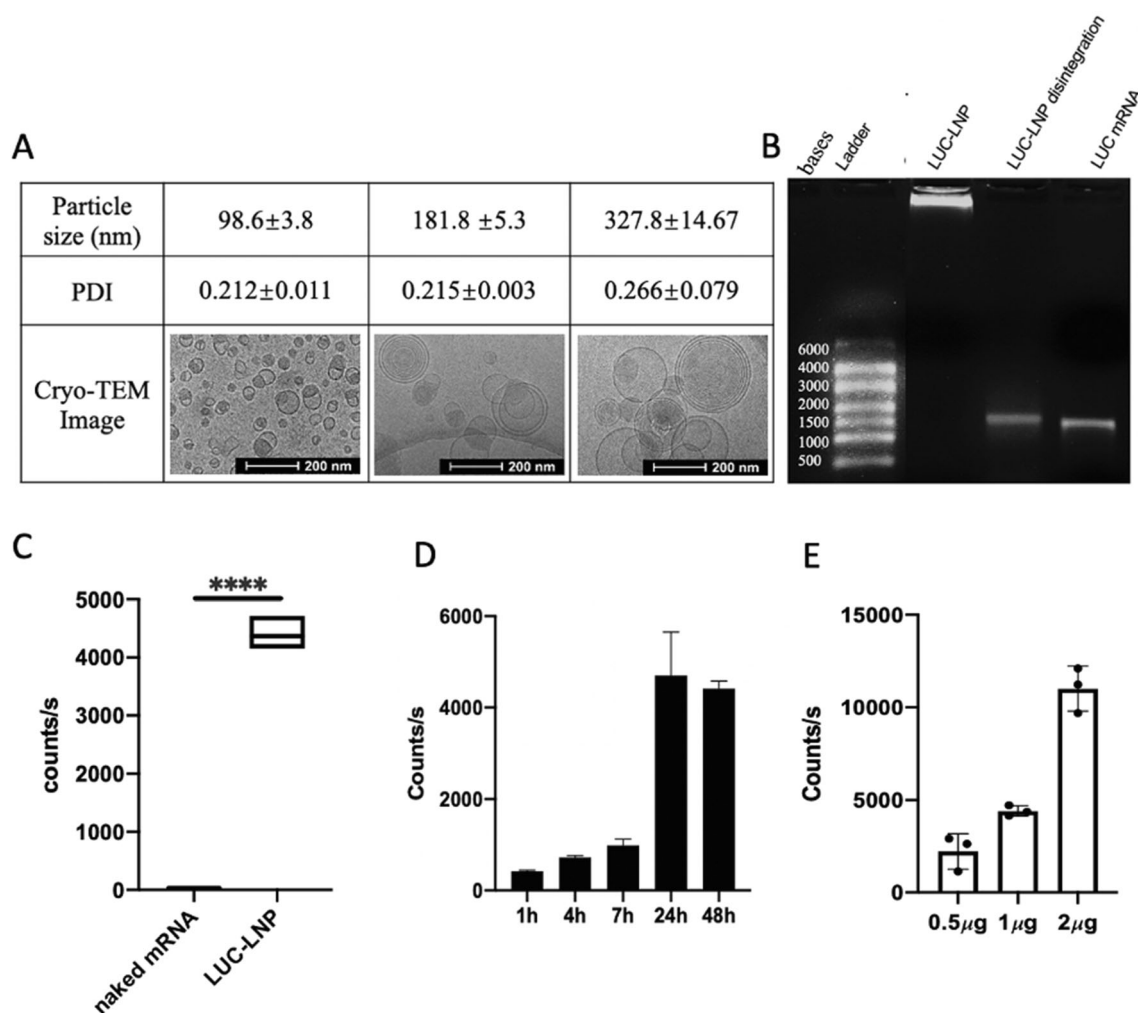


**Fig. 1** Physical and Biological evaluations of Fluc-mRNA LNPs. **(A)** Particle size distribution and cryo-TEM characterizations of LNPs prepared using three different mixing methods. **(B)** The mRNA LNPs evaluated by agarose gel electrophoresis. Lane 1: RNA ladder; lane 2: RNA-LNP; lane 3: RNA LNPs with Triton-X treatment; lane 4: naked mRNA. **(C)** Luciferase activities in HEK293T cells 24 h after mRNA transfection ( $1 \mu\text{g}$  mRNA per  $2.5 \times 10^5$  cells). The range of measurements are shown with a line indicating the mean. Statistical analysis was done using unpaired t-test. \*\*\*\*:  $p < 0.0001$ . **(D)** Luciferase activities measured at various time points after Fluc mRNA LNP transfection. Data are shown as mean  $\pm$  SD. **(E)** Luciferase activities after LNP transfection at different mRNA doses. Data are shown as mean  $\pm$  SD.

### Biodistribution of mRNA LNPs after Intramuscular Injection

The mRNA-LNPs were labeled physically by incorporating either the fluorescence dye, DiR, or deuterated cholesterol, and injected into the left leg muscle in mice. The distribution of fluorescence-labeled LNPs in live animals was imaged using an IVIS Spectrum (Fig. 2A). The fluorescent signals from several tissues of interest were measured by dissecting the specific tissues and ex vivo imaging. The fluorescence signal intensities from the injection site muscle, the draining lymph node, and liver and spleen were shown in Fig. 2B. Note that even with the wavelength used, the fluorescence intensity of internal organs could be significantly diminished due to light absorption and penetration limit in tissue depth. Based on the two measurements, the

fluorescence signals remained relatively constant within 48 h. Interestingly, the muscle signal increased over time to the highest at 48 h, while the liver signal went up to the most significant value at 7 h but became much smaller at 48 h. The DiR molecules incorporated in the LNPs likely leaked over time. Still, the steady signals at the injection site suggest such release might not be significant. In addition, metabolism and excretion of LNPs in liver might explain the signal decrease.

The biodistribution of deuterium-labeled LNPs was obtained by quantification using LC/MS. As shown in Fig. 2C, the highest concentration was measured at 2 h after the injection, indicating immediate exposure of the LNPs systemically. Shown as the ratio of the measured content to the administered dose, the blood content accounts for almost 15% of the injected amount. Given that deuterium-labeled cholesterol

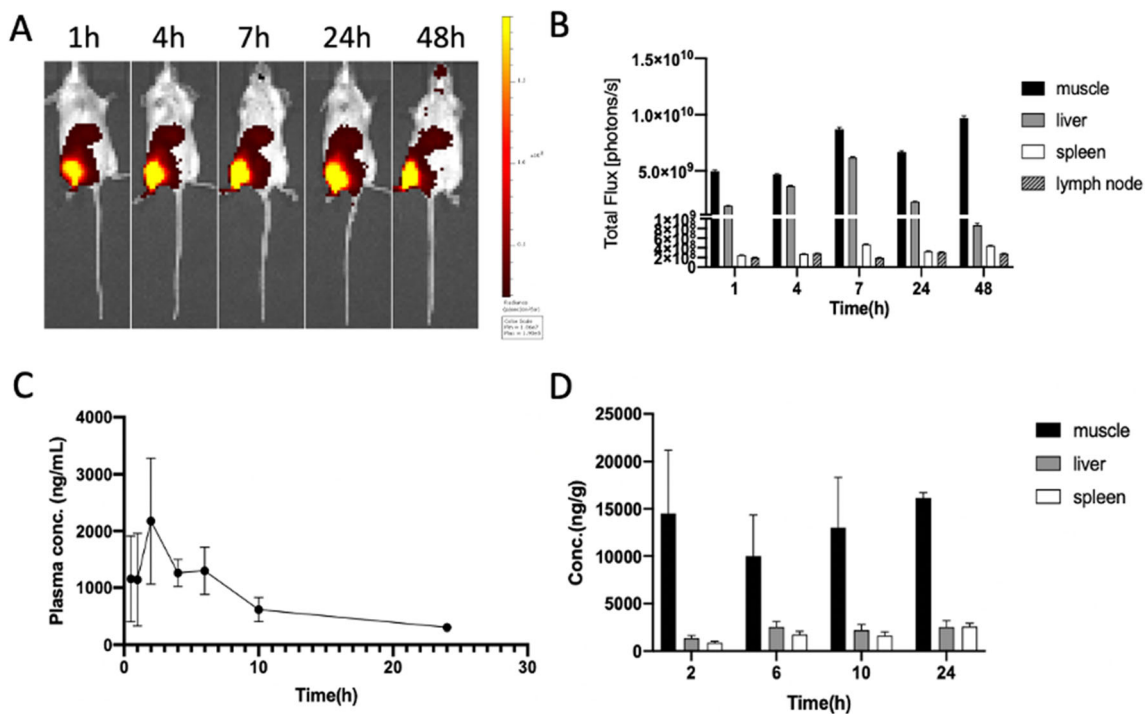


**Fig. 2** Measurements of the fluorescence label or deuterated cholesterol in mRNA-LNPs after intramuscular injection. Data are shown as mean  $\pm$  SD ( $n = 3$ ) unless specified otherwise. **(A)** Representative IVIS images at selected time points after DiR labeled mRNA-LNP injection. **(B)** Fluorescence signals of dissected tissues (liver, spleen, muscle, and inguinal lymph nodes) at specific time points. **(C)** Measurements of deuterated cholesterol labeled LNPs in the plasma samples after labeled LNP injection. **(D)** Measurements of deuterated cholesterol concentration in various tissue samples after labeled LNP injection.

are relatively stable inside the bilayer of the LNPs (13), released 2H-cholesterols could be minor in the plasma especially within the 2 h of injection. Figure 2D further illustrates the concentration measurements in tissue samples. The values agree well with the fluorescence intensity data in Fig. 2B, with the amount of LNPs in the muscle at the injection site being the highest and remaining relatively unchanged within 24 h. The liver and spleen show almost equivalent LNP concentrations. However, the volume of the liver is much larger than that of the spleen, thus the liver can capture more LNPs, as shown in Fig. 2B. Furthermore, When the concentration value is normalized to LNPs% per tissue, the muscle shows to accumulate 60–80% LNPs, the liver 10%–20%, and the spleen only 1%–2%.

Furthermore, the mRNA in the LNPs was examined in tissues and organs by *in situ* hybridization (Fig. 3). Muscle, liver, and the draining lymph nodes were collected 2 h after the intramuscular injection of LNPs containing OVAL mRNA. Tissue sections were stained with Cy5-labeled oligo probes. As shown in Fig. 3, faint mRNA signals were detected inside myocytes in the muscle from the injection site. The staining in the liver hepatocytes and lymphocytes in the draining lymph node was more clearly visible. The mRNAs were found isolated in individual hepatocytes aligning along liver sinusoids, while those in the lymph node were highly concentrated. It is possible that only released mRNAs could be stained and those inside

LNPs were not. Nevertheless, the results suggest that the transgenic efficiency was the largest in the lymph nodes.

### Luciferase Expression Resulted after I.M. Injection of mRNA LNPs

We examined luciferase expression in various tissues after the i.m. injection of mRNA LNPs and naked mRNAs. Figure 4 contained the bioluminescence images of the mice at different time points after injection. The naked mRNA injection only led to some luciferase expression at the injection site, while mRNA LNPs resulted in transfections in the liver. The bioluminescence imaging signals were quantified and plotted side by side in Fig. 4B. The LNP formulation delivered mRNA more efficiently, resulting in quicker and stronger gene expression at the injection site than naked mRNAs where the signal increased with time but remained relatively weaker.

In addition to these image-based analyses, we also collected blood and tissue samples for luciferase activity measurement *ex vivo* (Fig. 4B). Note that luciferase activities were normalized by tissue weight. As such, the liver had the highest transgene expression levels, more than the values in the muscle, which had a higher distribution of LNPs (Fig. 2). Even the spleen and lymph nodes demonstrated higher transfection efficiencies than the muscle, although they were too small to be seen in the live animal bioluminescence images (Fig. 4A). Only

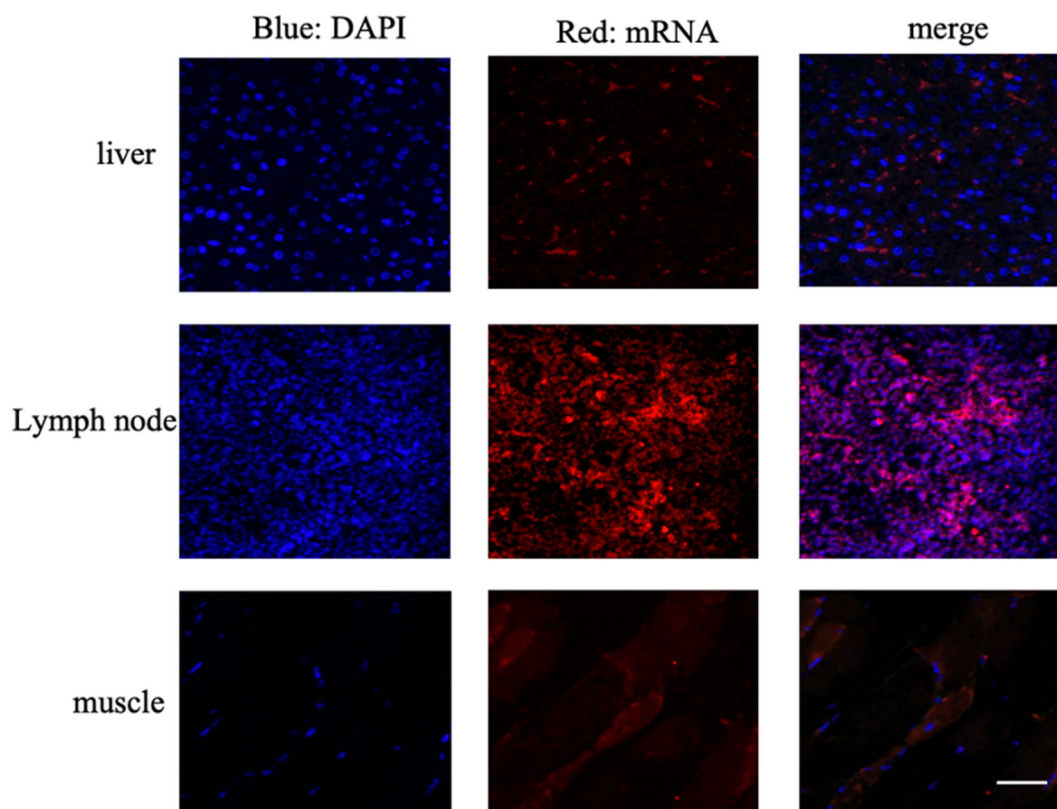


**Fig. 3** Fluorescence microscope images of tissue sections stained by *in situ* hybridization using Cy5 labeled mRNA sequence probes. The nuclei were stained with DAPI (blue). Images were taken in parallel using the same microscopy settings. Scale bar, 50  $\mu$ m.

the luciferase activity in the lymph node seemed to increase steadily with time. In other tissues, it peaked at 6–10 h after injection, and then the signal decreased.

#### Fluorescence-Labeled mRNA LNPs Distribution and Luciferase Expression in Mice after Administration Via Different Routes

The Fluc-mRNA LNPs were injected respectively via intramuscular, subcutaneous, and intravenous routes. The LNPs were physically labeled with the DiR dye. As shown in Fig. 5, intravenously injected LNPs led to particles accumulation mainly in the liver. The resulted luciferase expressions were also concentrated in the liver, as early as 1 h after injection. The bioluminescence peaked at 4 h and decreased quickly to almost background levels within 48 h after injection. mRNA LNPs were given intramuscularly led to delayed and weaker gene transfections at the injection site. Nonetheless, the protein expression in the liver was also significant. As aforementioned, fluorescence LNP signals remained mainly at the injection site for more than 72 h after injection. But the luciferase activities were no longer detectable after 48 h. In contrast, LNPs injected subcutaneously also remained at the injection site and the produced luciferase expression occurred locally at a much weaker degree.

#### Fluorescence-Labeled mRNA LNPs Distribution and Luciferase Expression in Mice Using LNPs with Different Sizes

Flu-mRNA LNPs with different size distributions were prepared as shown in Fig. 1A while maintaining the same lipid composition and mRNA to lipid ratios. They were injected into mice by intramuscular injection. Fluorescence and bioluminescence images at various time points are demonstrated in Fig. 6. Regarding the biodistribution of LNPs, particles with small particle sizes were more likely to migrate to the liver. In contrast, particles of large sizes mostly remained in the muscle tissue at the injection site. Interestingly, despite the dominant accumulation in the liver by the small LNPs, the luciferase activities in the liver were less significant than that of the medium-sized particles. The liver expression was much weaker for the larger particles, but the gene expression in the muscles was not affected.

## DISCUSSION

Lipid nanoparticles (LNPs) have been explored for delivering large biomolecules including proteins and RNAs (1,14). One siRNA LNP product was approved for the treatment of

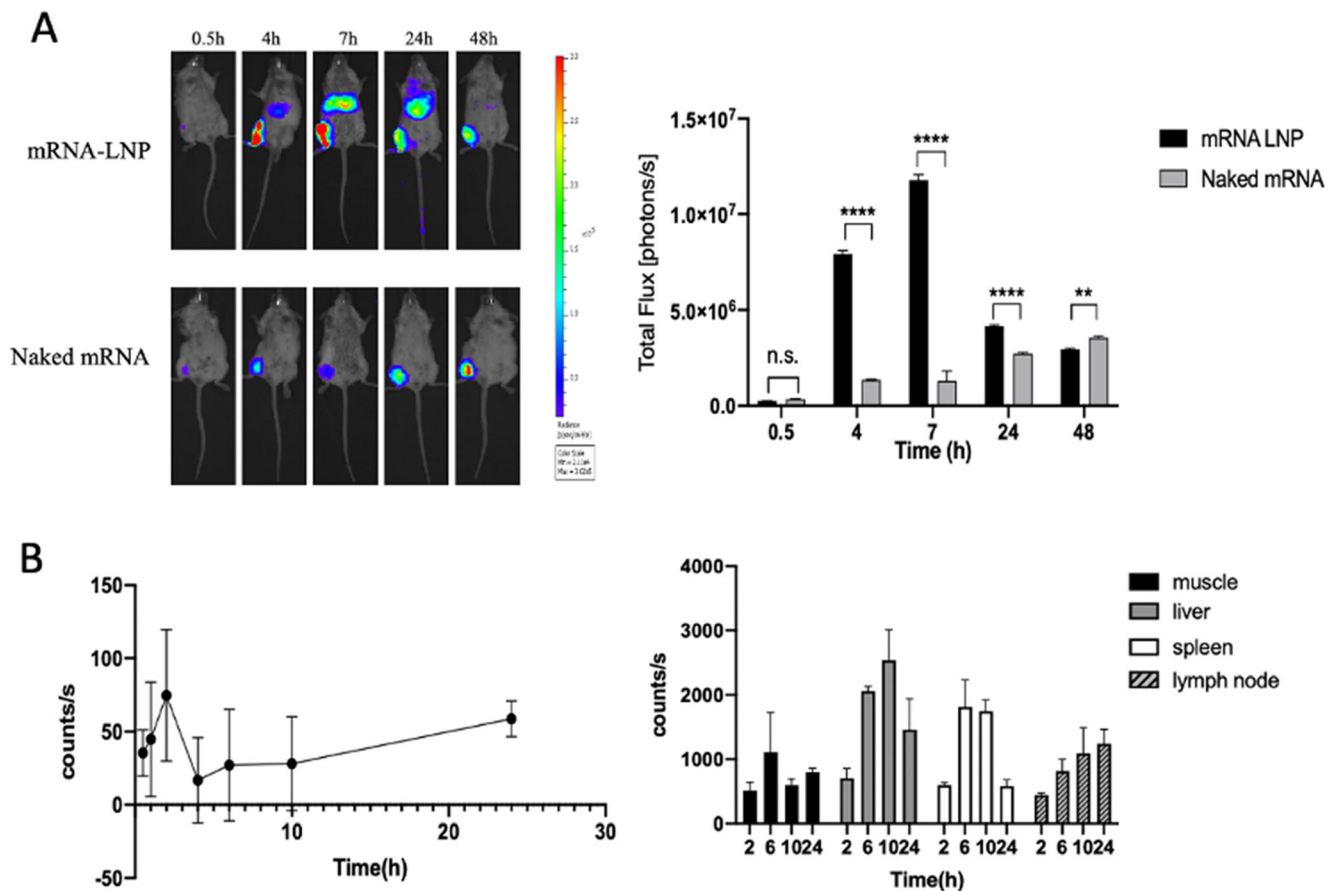


**Fig. 4** Luciferase expression after Fluc-mRNA LNP intramuscular injection in BALB/c mice ( $n = 3$ ). The injected mRNA dose was 10  $\mu$ g both the naked mRNA preparation and mRNA LNPs. **(A)** Representative IVIS images of the live animals and the fluorescence signal quantifications at the injection site. Data are shown as mean  $\pm$  SD ( $n = 3$ ). Statistical differences were evaluated using Students' t-test (n.s.: not significant; \*\*:  $p < 0.01$ ; \*\*\*\*:  $p < 0.0001$ ). **(B)** Measurements of luciferase activities in the blood (left) or tissues samples (right) obtained at various time points after mRNA-LNP injection. The luciferase signals were normalized by the total weight (gram) of tissues and shown as mean  $\pm$  SD ( $n = 3$ ).

transthyretin-mediated amyloidosis (15); LNPs carrying mRNAs are actively explored for cancer immunotherapy, protein replacement, and gene editing (16–18). It is reported that the magnitude and duration of transgene expression resulting from mRNA-LNPs vary significantly through different routes of administration (10). Intravenous, intraperitoneal, intramuscular, and intratracheal deliveries were shown leading to mRNA translation in the liver. This is confirmed by our study (Fig. 5). Nonetheless, the connection between the exposure of LNPs to the body and the immune response seems less explored with regard to delivery routes and nanoparticle properties. The purpose of this study was thereby to evaluate this relationship using a murine model.

LNP formulation generally contains similar components of ionizable lipids and co-lipids. The tertiary amine group of ionizable lipids is protonated around pH 4 and neutral at pH 7. The lipids are used to ensure a good balance between encapsulation integrity and intracellular delivery of the payload (e.g., mRNAs). By varying the mRNA concentration during mixing and the alcohol to buffer mixing ratios, three

different sizes of LNPs were prepared in this study (Fig. 1). The single-bilayer LNPs of our small batch was similar to the “blebs” reported (19,20), which was suggested as a bilayer construct with an amorphous electron-dense core doped by occasional electron-lucent cavities (21). Multi-layer structures were also found in our large LNP preparation. The mRNAs could not be clearly identified in the electron micrographs but likely reside between the layers. While the LNP microstructure may affect the LNP stability and possibly the transfection efficiency, we mainly focus on the role of the particle size on their biodistribution in this study. Given that there were different structures co-existing in these preparations, it would be ideal if one can isolate the different structures and evaluate their biodistribution and transfection activities respectively. Alternatively, we are also trying to adjust the mixing conditions to obtain preparations with more homogenous microstructures.

Intramuscularly injected LNPs were found in our study to migrate from the injection site and distribute into other organs and tissues. Luciferase activities and fluorescence were

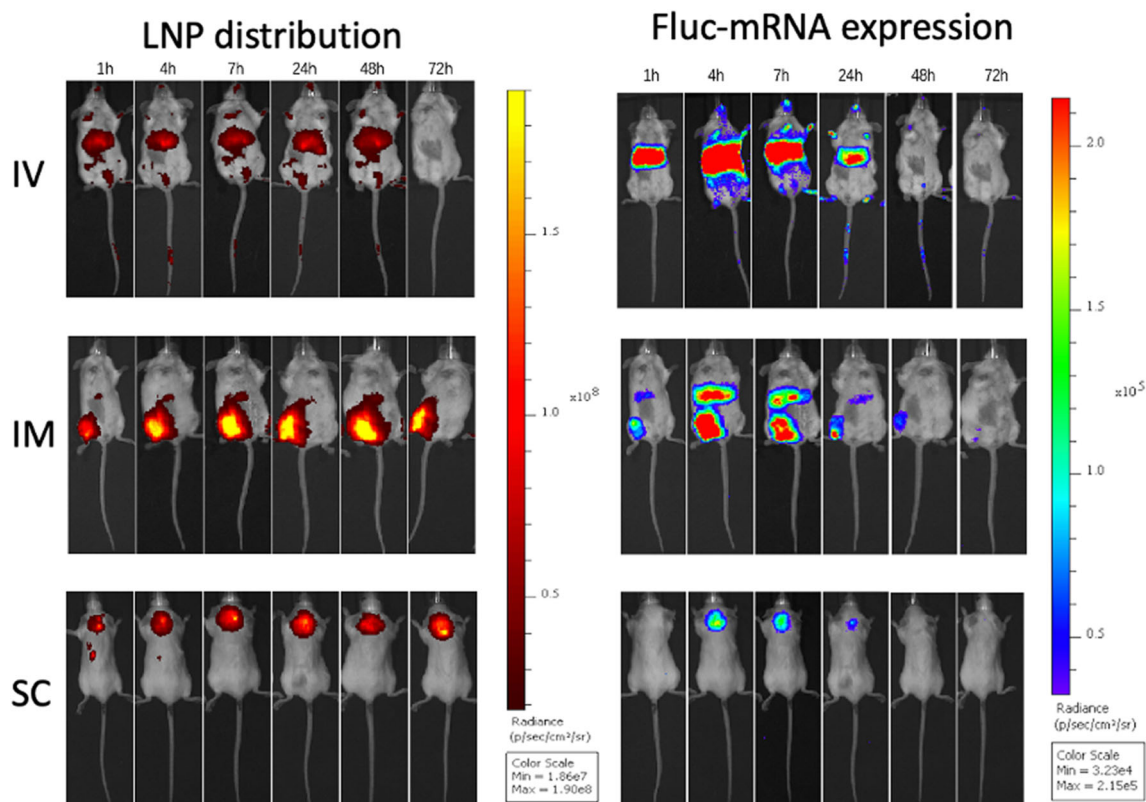


**Fig. 5** Biodistribution of DiR labeled Fluc-mRNA LNPs given via different routes of injection and the resulted luciferase expression signals. Representative images from one of the 3 mice per route of the injection group are shown. Both the fluorescence (left panel) images and bioluminescence (right) images were from the same mice taken using the same IVIS equipment.

detected in the liver and in the blood. A similar observation of mRNA expression in the liver is reported when negatively charged LNPs were given intramuscularly (21). In addition, Fig. 6 shows that smaller LNPs by intramuscular administration were relatively easier to be removed from the injection site than larger particles, possibly drained to lymph nodes. More concentrated mRNAs were found in the draining lymph nodes even for intramuscularly injected LNPs (Fig. 3), suggesting that lymphatic uptake is a major route prior to entering the systemic circulation. Nanoparticles smaller than 200 nm are believed to directly reach lymphatic drainage by advection (22–25), while particles between 200 and 500 nm may require dendritic cells (DCs) to circulate to the lymph (26). It is possible that both LNPs and transgene expression products were taken up by the lymphatic system and then into the blood circulation, corroborated by luciferase signals detected in blood samples even though luciferase usually are expressed intracellularly and not secreted (Fig. 4). Although we can not rule out the slim possibility that there might be needle damages to the blood vessel that caused LNPs and luciferase to spill over into the circulation. But the consistent detection of the LNPs and transgene products in the circulation suggests that mRNA LNPs and their activities in tissues other than the injection sites should be addressed for a complete evaluation of their safety and efficacy profiles.

Furthermore, it is found in this study that the biodistribution of LNPs was not linearly in agreement with the transgene expression by the encapsulated mRNAs due to the difference in the efficiency of mRNA release in tissues (Fig. 3). The distribution of LNPs in muscle tissues is more than three times that in liver when intramuscularly injected (Fig. 2). Yet, the mRNA expression efficacies were equivalent (Fig. 6). This indicates that even fewer LNPs captured in liver can result in a comparable amount of transgene proteins with that in muscles. The LNP exposure and the transgenic protein level were not linearly correlated. This non-linear relationship between the LNP exposure and the protein expression level varies in different tissues and organs. In addition, as shown in Fig. 6, even when more small particles could accumulate in the liver than the medium particles, the luciferase activities in the liver did not become stronger. Such difference could result from the size preference of endocytosis by cells.

Systemic exposure of mRNA-LNPs may lead to off-target expression of transgenes and elicit various adverse reactions including inflammation, allergic, hemolysis, etc. (27,28). The duration and kinetics of the transgene expression are affected by the PK and biodistribution of the delivery systems. The PK-PD relationship of mRNA LNPs is highly complex, making the prediction of gene expression and efficacy (PD) unlikely just based on the LNP exposures in tissue (PK).



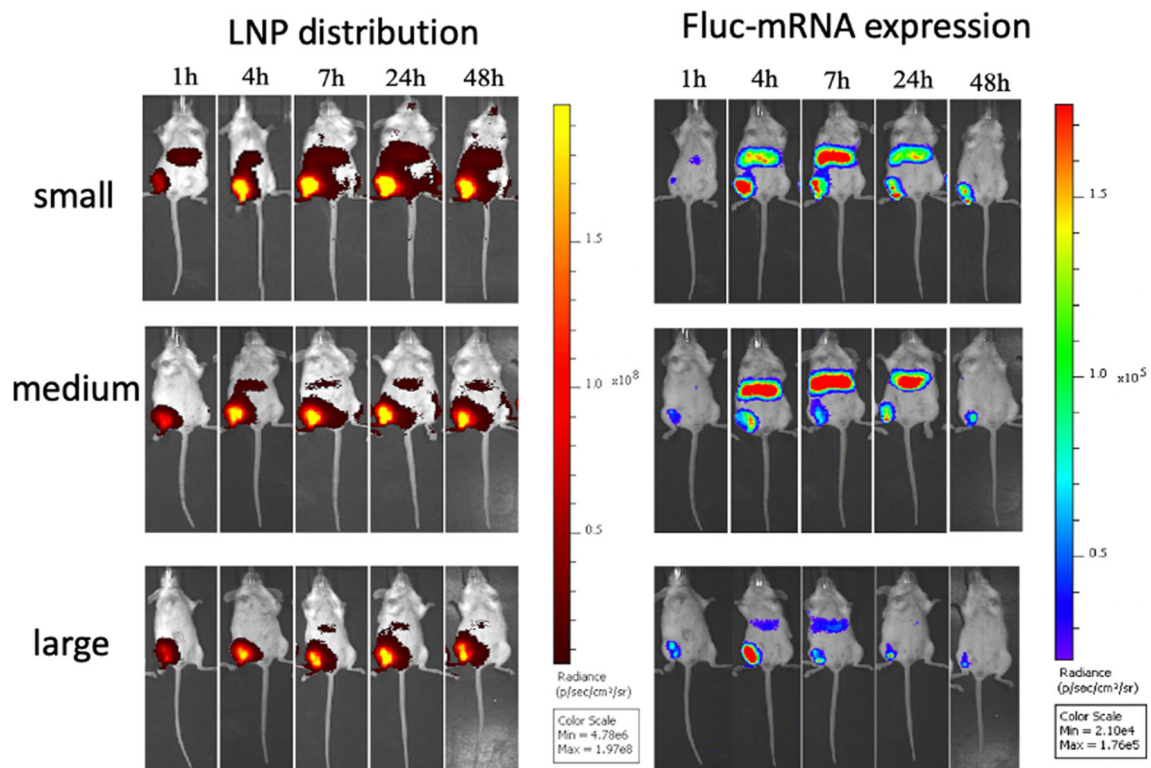


**Fig. 6** Biodistribution of DiR-labeled Fluc-mRNA LNPs with different size distribution and the resulted luciferase expression signals after intramuscular injection. Representative images from one of the 3 mice per size group are shown. Both the fluorescence (left panel) and bioluminescence (right) images were from the same mice taken using the same IMS equipment.

Nevertheless, it is prudent to fully characterize the PK in order to optimize the PD and minimize the toxicities of a gene delivery product (29,30).

## CONCLUSION

In this study, Fluc-mRNA was used as a model mRNA to be encapsulated in LNPs for studying the interplay between the LNP biodistribution and mRNA expression in tissues. Protein expression by the gene was imaged by bioluminescence and the biodistribution of the LNPs was attended by fluorescence imaging of encapsulated DiR molecules, as well as by chemical analysis of deuterated lipids in formulating the nanoparticles. It is discovered that LNPs after intramuscular injection were not wholly constrained in the muscle tissue but became rapidly distributed throughout the body with a large presence in the liver. Importantly, the tissue expression of released mRNAs was not linearly correlated with the LNP accumulation. The gene expression in the liver seemed quick and responsive. In contrast, the translation in the muscle was relatively slow but long-lasting. Furthermore, particle size and delivery route affected the LNP biodistribution and gene expression efficacy, and their non-linear, kinetic relationship.

**ACKNOWLEDGMENTS AND DISCLOSURES.** We thank Lingyun Wu in the Center of Cryo-Electron Microscopy (CCEM), Zhejiang University for her technical assistance on Cryo-EM. We are grateful for the technical support provided by HighField Biopharmaceuticals Corporation (Hangzhou, China). YX acknowledges the grant support from the National Natural Science Foundation of China (NSFC) No. 8169026. TL thanks Allen Chao Endowment. The authors report no conflicts of interest in this work.

**Data Availability** The datasets generated during the current study are available from the corresponding authors upon request.

## REFERENCES

1. Wu Z, Li T. Nanoparticle-mediated cytoplasmic delivery of messenger RNA vaccines: challenges and future perspectives. *Pharm Res.* 2021;38(3):473–8.
2. Schlake T, Thess A, Fotin-Mleczek M, Kallen K-J. Developing mRNA-vaccine technologies. *RNA Biol.* 2012;9(11):1319–30.
3. Weide B, Pascolo S, Scheel B, Derhovanessian E, Pflugfelder A, Eigntler TK, Pawelec G, Hoerr I, Rammensee HG, Garbe C. Direct injection of protamine-protected mRNA: results of a phase 1/2 vaccination trial in metastatic melanoma patients. *J Immunother.* 2009;32(5):498–507.

4. Blakney AK, McKay PF, Hu K, Samnuan K, Jain N, Brown A, *et al.* Polymeric and lipid nanoparticles for delivery of self-amplifying RNA vaccines. *J Control Release.* 2021;338:201–10.
5. Démoulin T, Milona P, Englezou PC, Ebensen T, Schulze K, Suter R, Pichon C, Midoux P, Guzmán CA, Ruggli N, McCullough KC. Polyethylenimine-based polyplex delivery of self-replicating RNA vaccines. *Nanomedicine.* 2016;12(3):711–22.
6. Xu Y, Zhang J, Liu J, Wang H, Ma X, Fang Z. Amphipathic derivatives of 3- (1- tert-butoxy carbonyl piperazines -4-yl) propionic acid and application thereof. CN105085437B. 2018.
7. Verbeke R, Lentacker I, De Smedt SC, Dewitte H. The dawn of mRNA vaccines: the COVID-19 case. *J Control Release.* 2021;333:511–20.
8. Meo S, Bukhari I, Akram J, Meo A, Klonoff D. COVID-19 vaccines: comparison of biological, pharmacological characteristics and adverse effects of Pfizer/BioNTech and Moderna vaccines. *Eur Rev Med Pharmacol Sci.* 2021;25(3):1663–9.
9. Schoenmaker L, Witzigmann D, Kulkarni JA, Verbeke R, Kersten G, Jiskoot W, Crommelin DJA. mRNA-lipid nanoparticle COVID-19 vaccines: structure and stability. *Int J Pharm.* 2021;601:120586.
10. Pardi N, Tuyishime S, Muramatsu H, Kariko K, Mui BL, Tam YK, Madden TD, Hope MJ, Weissman D. Expression kinetics of nucleoside-modified mRNA delivered in lipid nanoparticles to mice by various routes. *J Control Release.* 2015;217:345–51.
11. Hassett KJ, Higgins J, Woods A, Levy B, Xia Y, Hsiao CJ, Acosta E, Almarsson Ö, Moore MJ, Brito LA. Impact of lipid nanoparticle size on mRNA vaccine immunogenicity. *J Control Release.* 2021;335:237–46.
12. Meisel JW, Gokel GW. A simplified direct lipid mixing lipoplex preparation: comparison of liposomal-, dimethylsulfoxide-, and ethanol-based methods. *Sci Rep.* 2016;6(1):1–12.
13. Hanashima S, Ibata Y, Watanabe H, Yasuda T, Tsuchikawa H, Murata M. Side-chain deuterated cholesterol as a molecular probe to determine membrane order and cholesterol partitioning. *Organic & bioMolecular Chemistry.* 2019;17(37):8601–10.
14. Xu Y, Szoka FC. Mechanism of DNA release from cationic liposome/DNA complexes used in cell transfection. *Biochemistry.* 1996;35(18):5616–23.
15. Akinc A, Maier MA, Manoharan M, Fitzgerald K, Jayaraman M, Barros S, Ansell S, du X, Hope MJ, Madden TD, Mui BL, Semple SC, Tam YK, Ciufolini M, Witzigmann D, Kulkarni JA, van der Meel R, Cullis PR. The Onpatro story and the clinical translation of nanomedicines containing nucleic acid-based drugs. *Nat Nanotechnol.* 2019;14(12):1084–7.
16. Vlatkovic I. Non-immunotherapy application of LNP-mRNA: maximizing efficacy and safety. *Biomedicines.* 2021;9(5):530.
17. Cao J, An D, Galduroz M, Zhuo J, Liang S, Eybye M, Frassetto A, Kuroda E, Funahashi A, Santana J, Mihai C, Benenato KE, Kumarasinghe ES, Sabnis S, Salerno T, Coughlan K, Miracco EJ, Levy B, Besin G, *et al.* mRNA therapy improves metabolic and behavioral abnormalities in a murine model of citrin deficiency. *Mol Ther.* 2019;27(7):1242–51.
18. Muhar M, Ebert A, Neumann T, Umkehrer C, Jude J, Wieshofer C, Rescheneder P, Lipp JJ, Herzog VA, Reichholf B, Cisneros DA, Hoffmann T, Schlapanzky MF, Bhat P, von Haeseler A, Köcher T, Obenauf AC, Popow J, Ameres SL, Zuber J. SLAM-seq defines direct gene-regulatory functions of the BRD4-MYC axis. *Science.* 2018;360(6390):800–5.
19. Brader ML, Williams SJ, Banks JM, Hui WH, Zhou ZH, Jin L. Encapsulation state of messenger RNA inside lipid nanoparticles. *Biophys J.* 2021;120(14):2766–2770.
20. Kulkarni JA, Darjuan MM, Mercer JE, Chen S, Van Der Meel R, Thewalt JL, *et al.* On the formation and morphology of lipid nanoparticles containing ionizable cationic lipids and siRNA. *ACS Nano.* 2018;12(5):4787–95.
21. Carrasco MJ, Alishetty S, Alameh M-G, Said H, Wright L, Paige M, Soliman O, Weissman D, Cleveland TE IV, Grishaev A, Buschmann MD. Ionization and structural properties of mRNA lipid nanoparticles influence expression in intramuscular and intravascular administration. *Commun Biol.* 2021;4(1):1–15.
22. Chen S, Tam YYC, Lin PJ, Leung AK, Tam YK, Cullis PR. Development of lipid nanoparticle formulations of siRNA for hepatocyte gene silencing following subcutaneous administration. *J Control Release.* 2014;196:106–12.
23. Oussoren C, Zuidema J, Crommelin D, Storm G. Lymphatic uptake and biodistribution of liposomes after subcutaneous injection.: II. Influence of liposomal size, lipid composition and lipid dose. *Biochimica et Biophysica Acta (BBA)-Biomembranes.* 1997;1328(2):261–72.
24. Oussoren C, Storm G. Liposomes to target the lymphatics by subcutaneous administration. *Adv Drug Deliv Rev.* 2001;50(1–2):143–56.
25. Gao X, Voronin G, Generaux C, Rose A, Kozhich A, Dalglish G, Rosa R, Oh S, Kagan L. Lymphatic distribution of Etanercept following intravenous and subcutaneous delivery to rats. *Pharm Res.* 2020;37(8):1–8.
26. Bachmann MF, Jennings GT. Vaccine delivery: a matter of size, geometry, kinetics and molecular patterns. *Nat Rev Immunol.* 2010;10(11):787–96.
27. Walsh EE, Frenck R, Falsey AR, Kitchin N, Absalon J, Gurtman A, *et al.* RNA-based COVID-19 vaccine BNT162b2 selected for a pivotal efficacy study. *Medrxiv.* 2020;383(25):243–2450
28. Anderson EJ, Rouphael NG, Widge AT, Jackson LA, Roberts PC, Makhene M, Chappell JD, Denison MR, Stevens LJ, Pruijssers AJ, McDermott A, Flach B, Lin BC, Doria-Rose NA, O'Dell S, Schmidt SD, Corbett KS, Swanson PA 2nd, Padilla M, Neuzil KM, Bennett H, Leav B, Makowski M, Albert J, Cross K, Edara VV, Floyd K, Suthar MS, Martinez DR, Baric R, Buchanan W, Luke CJ, Phadke VK, Rostad CA, Ledgerwood JE, Graham BS, Beigel JH, mRNA-1273 Study Group Safety and immunogenicity of SARS-CoV-2 mRNA-1273 vaccine in older adults. *N Engl J Med.* 2020;383(25):2427–2438.
29. Hawthorne G, Henderson N, Hölttä M, Khan S, Lindqvist J, Wilson A. Overcoming analytical challenges to generate data critical to understanding lipid nanoparticle-delivered modified mRNA biodistribution. *Bioanalysis.* 2019;11(21):1993–2001.
30. Reiser A, Woschée D, Mehrotra N, Krzysztoń R, Strey H, Rädler J. Correlation of mRNA delivery timing and protein expression in lipid-based transfection. *Integr Biol.* 2019;11(9):362–71.

**Publisher's Note** Springer Nature remains neutral with regard to jurisdictional claims in published maps and institutional affiliations.